Chromogranin B (CHGB): Intra- and extra-cellular mechanisms to regulate catecholamine storage and release, in catecholaminergic cells and organisms

Kuixing Zhang, MD/PhD[*], **Nilima Biswas, PhD**[*], **Jiaur R. Gayen, PhD**, **Jose Pablo Miramontes-Gonzalez, MD/PhD**, **C. Makena Hightower, PhD**, **Maja Mustapic, PhD**, **Manjula Mahata, PhD**, **Chun-Teng Huang, PhD**, **Vivian Y. Hook, PhD**, **Sushil K. Mahata, PhD**, **Sucheta Vaingankar, PhD**, and **Daniel T. O'Connor, MD**

Departments of Medicine and Pharmacology, and Institute for Genomic Medicine (IGM), University of California at San Diego, La Jolla, CA, and VA San Diego Healthcare System, La Jolla, CA

Abstract

CHGB is the major matrix protein in human catecholamine storage vesicles. *CHGB* genetic variation alters catecholamine secretion and blood pressure. Here effective Chgb protein under-expression was achieved by siRNA in PC12 cells, resulting in ~48% fewer secretory granules on EM, diminished capacity for catecholamine uptake (by ~79%), and a ~73% decline in stores available for nicotinic cholinergic-stimulated secretion. *In vivo*, loss of *Chgb* in knockout mice resulted in a ~35% decline in chromaffin granule abundance and ~44% decline in granule diameter, accompanied by unregulated catecholamine release into plasma. Over-expression of *CHGB* was achieved by transduction of a *CHGB*-expressing lentivirus, resulting in ~127% elevation in CHGB protein, with ~122% greater abundance of secretory granules, but only ~14% increased uptake of catecholamines, and no effect on nicotinic-triggered secretion. Human CHGB protein and its proteolytic fragments inhibited nicotinic-stimulated catecholamine release by ~72%. One conserved-region CHGB peptide inhibited nicotinic-triggered secretion by up to ~41%, with partial blockade of cationic signal transduction. We conclude that bi-directional quantitative derangements in CHGB abundance result in profound changes in vesicular storage and release of catecholamines. When processed and released extra-cellularly, CHGB proteolytic fragments exert a feedback effect to inhibit catecholamine secretion, especially during nicotinic cholinergic stimulation.

Keywords

Chromogranin B; hypertension; adrenal; chromaffin; catecholamines

Correspondence to: Daniel T. O'Connor MD, Sucheta Vaingankar PhD, or Sushil K. Mahata PhD, Department of Medicine and IGM, UCSD School of Medicine, 9500 Gilman Drive, La Jolla, CA 92093-0838. Telephone: (858)-5340661. Fax: (858)-5340626. <doconnor@ucsd.edu>, <svaingankar@ucsd.edu> or <smahata@ucsd.edu>. Internet: <http://medicine.ucsd.edu/hypertension>.
[*]Equal contributions.

Conflicts of interest: None to declare.

INTRODUCTION

The sympathetic branch of the autonomic system exerts minute-to-minute control over the circulation. Sympathoadrenal catecholamine secretion is exocytotic (all-or-none), releasing not just catecholamines but also the proteins with which catecholamines are co-stored. The chromogranins/secretogranins comprise a family of acidic, soluble proteins that are widely stored in secretory granules with hormones, transmitters, and neuropeptides throughout the endocrine and nervous systems ([1,2]). Chromogranin B (CHGB), first described in the 1980s, ([3,4]) seems to be the quantitatively most abundant matrix protein in the core of human catecholamine storage vesicles ([5,6]). Expression studies in chromaffin cells suggest that CHGB plays a functional role in secretory vesicle biogenesis ([7]).

CHGB may have both extra-cellular and intra-cellular roles in the neuroendocrine system. Extracellular roles for CHGB are dependent on its proteolytic processing within secretory granules ([8]) to form smaller peptides; such peptides may have a role in the neuroendocrine/ sympathoadrenal stress response to systemic infection ([2]), and CHGB fragments may also play an autocrine inhibitory role on the release of co-stored hormones, such as insulin ([9]). Within chromaffin cells and sympathetic axons,CHGB functions in sorting and trafficking of peptide hormone and neuropeptide precursors to secretory granules ([10]), perhaps as triggers to secretory granulogenesis ([7]).

Hypertension is a complex trait in which deranged autonomic control of the circulation may be an early etiological culprit ([11]). Expression of *CHGB* may mark the action of QTLs (including the *CHGB* locus itself) influencing exocytotic sympathoadrenal activity ([12,13]). *CHGB* is over-expressed in rodent models of genetic ([14,15]) as well as acquired ([16]) hypertension, thus suggesting augmented sympathoadrenal activity in the pathogenesis of these syndromes. Therefore *CHGB* gives rise to early, pathogenic "intermediate phenotypes" ([17]) for exploration of sympathoadrenal activity in human essential hypertension. Indeed, we reported that two common *CHGB* promoter SNPs, A-296C (rs236140) and A-261T (rs236141), are strongly associated with hypertension in the population ([18,19]), while in *CHGB* knockout (*CHGB^{−/−}*) mice, we observed substantial elevations in both SBP and DBP ([18]). In this report, we have studied how *CHGB* quantitative variation (both over- and under-expression) affects not only secretory granulogenesis, but also catecholamine uptake, storage, and exocytotic release. We also describe the effects of novel CHGB fragments upon catecholamine release and its nicotinic cholinergic signal transduction pathway.

METHODS

Chromaffin cell biology

Rat pheochromocytoma (PC12) cells were cultured in a medium containing DMEM with high glucose (cat#: 11965, Invitrogen), 10% horse serum, 5% fetal bovine serum (FBS) and 1x penicillin/streptomycin/glutamine. The cells were cultured in an incubator with 6% CO_2 at 37°C, and cell passage number (since initiation of the line) was between 10 and 25 in these experiments.

Secretion of catecholamines from chromaffin cells

Norepinephrine secretion from PC12 cells was assayed as described previously ([20]). After washing, cells treated with nicotine (60 μM; for nicotinic cholergic stimulation) or KCl (55 mM; for membrane depolarization) in physiological secretion medium. Each experiment was repeated three times.

Transmission electron microscopy (EM)

TEM on cells/tissues was conducted as previously described ([21]).

Silencing CHGB expression by small interfering RNA (siRNA) in PC12 cells

We used a rat *CHGB* siRNA siGENOME "smart pool" (Cat# M-099320-00, Dharmacon). One day before transfection, PC12 cells were grown on poly-l-lysine-coated 12-well plates and transfected for 48 h with 30, 15 or 7.5 nmol/well siRNA using the Transfectin reagent (BioRad). Silencing of *CHGB* expression was evaluated by immunoblotting at the protein level and real time PCR at the mRNA level. A control siRNA (Cat#: D-001210-01-05, Dharmacon) pre-designed to minimize off-target effects was used as a transfection negative control. The effect of reduced expression of *CHGB* on dense-core secretory granule abundance was examined by transmission electron microscopy (EM). The anti-CHGB antibody (C-19; catalog #:sc-1489, Santa Cruz Biotechnology) was a goat polyclonal IgG (provided at 200 μg/ml, and used at 1:3000) for detecting CHGB of rat or human origin.

CHGB ablation *in vivo*: Knockout mice, transmission EM, and catecholamine release

Mouse studies were conducted with the approval of the UCSD Animal Subjects Committee, and the ARRIVE guidelines were followed. *CHGB* knockout mice were generated from mouse embryonic stem cells by homologous recombination, as previously described ([18,22]). The effect of *CHGB* knockout on dense-core secretory granule abundance was examined by transmission electron microscopy (EM). Plasma catecholamines were investigated by high performance liquid chromatography coupled to an electrochemical detection (HPLC-ECD) system.

Over-expression of CHGB in PC12 cells by transduction of a *CHGB* lentivirus

Human cDNA clone h*CHGB*-pCMV6XL5 (Cat#: SC119004, Origene, Rockville, MD) was used as template. The 5′ primer, 5'- agcCCCGGGatgcagccaacgctgcttct -3', includes a *SmaI* site (capitalized), while the 3′ primer, 5′- caaGTCGACtcagccccctttggctgaatt -3', includes a *SalI* site (capitalized). The 2034 bp PCR product was digested with SmaI and SalI (New England Biolab), purified (Cat#: 28074, Qiagen), and ligated into corresponding site of SIN18-hPGK-tdTomato-T2A vector to generate SIN18-hPGK-tdTomato-T2A-hCHGB lentiviral vector plasmid (Supplementary Figure 1). The SIN18-hPGK-tdTomato is used as control lentiviral vector.

The standard operation procedure of lentivirus production is as described ([23]). Briefly, three plasmids (the lentiviral vector plasmid, the packaging plasmid pCMVDR8.74, and the vesicular stomatitis virus (VSV) glycoprotein expression plasmid pMD.G) are mixed in a ratio of 3:2:1 for transient transfection into HEK-293T cells using the calcium phosphate

method. Un-concentrated viral supernatant is collected every 24 hours up to 4 days post-transfection, and a commercially available serum-free ultraculture medium (Bio-Whitttaker #12-725F) with 1 mM L-glutamine, 50 U/mL penicillin, and 50 mg/mL streptomycin is used to refeed the transfected plate. The pooled viral supernatant is filtered through 0.22 μm pores, followed by concentration and purification by 20% sucrose gradient centrifugation at 21,000 rpm for 2 hours. The viral lysate is resuspended in 1x HBSS (Hank's Balanced Salt Solution), followed by flow cytometry titration in 293T cells.

For lentiviral transduction, concentrated viral supernatant was added into PC12 cells at a MOI of 0.5, and incubated at 37 °C overnight. Cells were subjected to culture, experiment, or analysis 72 hours post-transduction.

Flow cytometry

PC12 cells grown on 100-mm plates and infected with the lenti-hPGK-tdTomato-T2A-h*CHGB* or lenti-hPGK-tdTomato-T2A control viruses, were suspended in Accutase detachment solution (Innovative Cell Technologies) at a concentration of 2×10^6 cells/ml. Cells (7×10^6/sample) were analyzed for tdTomato fluorescence using a MoFlo cell sorter (DakoCytomation). Fluorescence-activated cell sorting (FACS) achieved the isolation of lentivirus-infected cells. An aliquot of each cell sample was processed for immunocytochemistry (anti-HA monoclonal antibody) to evaluate the expression of *CHGB*, and the remaining cells were processed for characterization by biochemistries and imaging by TEM.

Prokaryotic expression and purification of CHGB: pET-hCHGB-6-His

Human *CHGB* cDNA encoding the mature protein (minus the 20-residue signal peptide) was excised by PCR from the eukaryotic expression plasmid h*CHGB*-pCMV6XL5 (Cat#: SC119004, Origene, Rockville, MD) as template. The 5′ primer, 5'-gtcCATATGatgccagtggataacaggaa-3' is preceded by a *Nde*I site (capitalized) and the 3′ primer, 5′-tgaGTCGACgcccctttggctgaatttct-3', is preceded by a *Sal*I site (capitalized). The PCR product was digested with NdeI and SalI (New England Biolab) and gel-purified (Cat#: 28074, Qiagen). The resulting fragment of 1974 base pairs was directionally cloned into the expression vector, pET-21a-d (Novagen, Madison, WI). The final construct was designated to encode the mature (i.e., minus signal peptide) human CHGB (657 residues) with addition of the residues VDKLAAALEHHHHHH at the carboxy-terminus (thus a total of 682 residues for the final recombinant protein). The nucleotide sequences of the PCR products and the junction regions between the insert and the vector were verified from both strands by direct dideoxy-capillary sequencing.

BL21(DE3)pLysS (Novagen, Madison, WI) competent E.coli were transformed with the pET-(hCHGB-6-His) plasmid. Cells were induced with IPTG (isopropyl β-D-thiogalactopyranoside; 1 mM), and grown in LB broth containing ampicillin (50 μg/ml) at 37°C until an A_{600} of ~0.8 was reached. The recombinant protein was purified as described previously using its 6-His affinity tag ([24]). Protein concentration was determined by Bio-Rad protein assay reagent (Bio-Rad Laboratories, Hercules, CA). Aliquotted protein was stored at −70°C until further use.

Endoproteolytic cleavage of CHGB

Plasmin is serine protease found in chromaffin cells that can process CHGA to its bio-active catestatin fragment ([25–27]). In order liberate a "catestatin-like" peptide from CHGB, we thus turned to plasmin as a protease. Purified human recombinant CHGB protein (10 μmol/reaction) was incubated with human plasmin (EC_3.4.21.7, 2 μmol/reaction; Calbiochem catalog #527624; specific activity 10 U/mg protein) in digestion buffer (10 mM Tris-HCl, pH 8.0; 0.15 M NaCl) at 37°C for 30 min. The reaction was terminated by the addition of aprotinin (2.5 μM). For secretion assay, the cells were treated with nicotine (60 μM) in secretion medium, either alone or in combination with recombinant CHGB (3.0 μM) full-length, or pre-digested by plasmin. The digestion reaction (1 hr) contained CHGB (10 μM) and plasmin (2 μM) in a reaction volume of 120 μl of 10 mM Tris-Cl, pH 8.0 and NaCl 150 mM. After digestion, peptides were purified (and intact plasmin removed) by C18 cartridge (Waters, Milford, MA), lyophilized, and suspended in water.

LC-MS/MS

In one experiment, plasmin-digested human CHGB (without added aprotinin) was subjected to LC-MS/MS, for identification of cleavage sites. Plasmin-digested peptides were analyzed by HPLC coupled to tandem mass spectroscopy (LC-MS/MS) using nanospray ionization, in a Triple TOF 5600 hybrid mass spectrometer (AB-SCIEX) interfaced with nano-scale reversed-phase HPLC (Tempo) using a 10 cm-100 micron ID glass capillary packed with 5-μm C-18 ZorbaxTM beads (Agilent Technologies, Santa Clara, CA). Peptides were eluted from the C18 column into the mass spectrometer using a linear gradient (5–60%) of ACN (acetonitrile) at a flow rate of 250 μl/min for 1hr. The buffers used to create the ACN gradient were: Buffer A (2% ACN, 0.2% formic acid, and 0.005% TFA, in H2O) and Buffer B (0.2% formic acid, and 0.005% TFA in ACN). MS/MS data were acquired as follows: MS-1 data were obtained for 250 ms at m/z of 400 to 1250 Da, while MS-2 data spanned m/z of 50 to 2,000 Da. The independent data acquisition (IDA) parameters were: MS-1 TOF 250 milliseconds, followed by 50 MS-2 events of 25 milliseconds each, and IDA criteria of over 200 counts (threshold) and charge state +2 to +4, with a 4 second exclusion. Finally, collected data were analyzed by MASCOT® (Matrix Sciences) and Protein Pilot 4.0 (AB-SCIEX) for peptide sequence identification, with reference to the human CHGB amino acid sequence as template (UniProt P05060, NCBI NP_001810).

CHGB peptide synthesis

Five peptides were synthesized by solid-phase F-moc chemistry, with molecular mass verified by electrospray mass spectrometry (Mimotopes; Minneapolis, MN). CHGB regions were selected for a preponderance of sequence features bearing similarity to the catecholamine release-inhibitory CHGA fragment catestatin (human CHGA[352–372]) ([28,29]): basic isoelectric point (pI), basic amino acids (Arg, Lys; including dibasic or tribasic sites), hydrophobicity or aromaticity (Leu, Ile, Val, Phe, Tyr, His); amphiphilicity (alternating hydrophobic and cationic residue side chains); and relative abundance of the product after cleavage out of the CHGB precursor in chromaffin granules *in vivo* ([30–32]). The synthetic sequences were: hCHGB[60–67], KFEVRLLR; hCHGB[259–272], TRPRHHHGRSRPDR; hCHGB[337–354], LEWERYRGRGSEEYRAPR; hCHGB[389–

419], RGLEPGKGRHHRGRGGEPRAYFMSDTREEKR; and hCHGB[480–497],
RFQDKQYSSHHTAEKRKR.

Nicotinic cholinergic signal transduction: $^{45}Ca^{2+}$ uptake

PC12 cells were seeded onto poly-L-lysine–coated six-well polystyrene culture dishes 2
days before study. Cells were rinsed with 1 ml of secretion buffer (150 mM NaCl, 5 mM
KCl, 2 mM $CaCl_2$, 10 mM Hepes, pH 7.4) every 15 minutes for 1 hour at 37°C.
Then $^{45}Ca^{2+}$ was added (2 μCi/ml, 14.95 mCi/mg, DuPont-NEN)) to Ca^{2+}-free buffer
(secretion buffer without 2 mM $CaCl_2$), and drugs were to the labeled buffer at 37°C. The
cells were incubated with labeled buffer under different conditions for 5 minutes at room
temperature. Calcium uptake was stopped simultaneously in all six wells by inversion of the
plate, so all wells were decanted together, followed by prompt addition of ice-cold release
buffer containing 2 mL of 1 mmol/L $LaCl_3$ for termination of further uptake of extracellular
labeled calcium. The culture dishes were then rinsed twice with ice-cold release buffer. One
ml of cell lysis buffer was added to cells in each well and collected for liquid scintillation
counting. The data were expressed as counts per minute per well.

Statistical Analyses

Results are expressed as mean ± 1 SEM (standard error of the mean). The reported "n"
refers to the number of replications. Data were evaluated by Student t test or ANOVA,
followed by post hoc tests, in Excel (Microsoft, Bellevue, WA) or SPSS-17 (Chicago, Ill). P
values <0.05 were considered statistically significant.

RESULTS

Silencing *CHGB* expression in chromaffin cells by siRNA

Introduction of rat *CHGB* siRNA into PC12 dose-dependently decreased CHGB protein
expression on immunoblot. *CHGB* siRNA knocked down CHGB protein by 81% (p=0.02) at
7.5 nM and >95% at 15 nM (p=0.01, Figure 1a). In the catecholamine storage/synthesis
pathway, after *CHGB* siRNA treatment real-time qPCR indicated that *CHGB* mRNA
declined by 46% (p<0.05), while these mRNAs increased: *Chga* (by 35% p<0.05); and *Dbh*
(by 243%, p=0.003). There were no changes in mRNAs encoding *Scg2* or *Th* (Figure 1b).
The increase in *Dbh* transcription suggests negative feedback control by cellular
catecholamine content, but the mechanism of such an effect is not established.

Effect of *CHGB* siRNA knockdown on catecholamine storage, uptake, or secretion in chromaffin cells

After *CHGB* siRNA, transmission electron micrographs indicated a ~48% less of dense core
granule abundance in *CHGB* siRNA treated PC12 cells compared to control cells (Figure
1c). There were 25.4±2.7 granules per 100 μm^2) in control PC12 cells and 13.3±2.5 granules
per 100 μm^2 in *CHGB* siRNA PC12 cells (p=0.006, Figure 1d left). Average granule
diameter was 63.4±2.75 nm after *CHGB* siRNA, versus 92.8±1.87 nm in control cells, thus
declining by ~32% during knockdown (p<0.001, Figure 1d right). Uptake of exogenous
catecholamines in *CHGB* siRNA-silenced cells declined by ~78% compared to control
(p<0.0001, Figure 1e). Secretion of catecholamines during nicotinic cholinergic stimulation

also declined by ~75% (p=0.005, Figure 1e). Basal secretion of catecholamine was also diminished in *CHGB* siRNA-silenced cells (p=0.023, Figure 1e).

CHGB targeted ablation *in vivo*: *CHGB* knockout mice

Morphology (transmission EM of the adrenal medulla)

Transmission EM indicated that dense core granules in the adrenal medulla of *CHGB*(−/−) mice displayed both loss of abundance and decline in size. In *CHGB* knockout mice, the number of granules was 9.1±0.55 per μm^2 in *CHGB*(+/+) mice versus 5.9±0.59 per in *CHGB*(−/−) mice, thus declining by ~35% (p<0.001, Figure 2a). The average diameter of dense core granules was 173.1±6.3 nm in *CHGB*(+/+) mice, declining by ~44% to 97.4±3.6 in *CHGB*(−/−) mice (p<0.001, Figure 2a).

Catecholamine secretion *in vivo*

Here we found that plasma concentratios of both norepinephrine and epinephrine were significantly higher in *CHGB* knockout mice, with norepinephrine increasing from 22.6±3.4 to 36.9±4.2 ng/ml in *CHGB*(−/−) mice, and epinephrine from 8.1±0.9 to 14.7±2.2 ng/ml: increments of ~1.6-fold for norepinephrine and ~1.7-fold for epinephrine (each p<0.05, Figure 2b).

Over-expression of *CHGB* in chromaffin cells by lentivirus transduction

After transduction by *CHGB*-lentivirus, over-expressing PC12 cells were selected by flow cytometry based on the tdTomato photoprotein red fluorescence (Supplemental Figure 2). Transduction caused an increase of CHGB protein by ~127% compared to control cells (Figure 3a), while the abundance of dense core granules increased from 22.2±4.4 per high-power field (2.0×10^{-10} m^2) in control cells to 50.3±8.3 in virus-infected cells (P=0.01, Figure 3b and 3c). The diameter of granules was unchanged, at 92.8±1.87 nm in control cells versus 90.9±2.98 nm in *CHGB* over-expressing cells. Over-expression of CHGB caused increased exogenous catecholamine uptake by ~14% (p=0.019), but did not alter nicotinic cholinergic stimulation of catecholamine release (p>0.05, Figure 3d).

Extra-cellular effects of CHGB and its proteolytic fragments: Catecholamine release from chromaffin cells

Both intact CHGB itself and its plasmin-digested fragments inhibited nicotinic cholinergic-stimulated catecholamine release, with ~53% reduction by CHGB itself and ~72% reduction by its fragments (p<0.01, Figure 4A, left). By contrast, CHGB or its fragments only moderately inhibited membrane depolarization-stimulated catecholamine release: ~23% reduction by CHGB and ~32% by its proteolytic fragments (p<0.01, Figure 4A, right).

Screening CHGB peptides for inhibition of nicotinic cholinergic secretion

The 5 synthetic CHGB peptides displayed a spectrum of inhibitory effects on nicotinic cholinergic secretion, with the shortest fragment CHGB[60–67] (KFEVRLLR) exerting the most prominent effect, reducing nicotinic stimulation's effect by ~41%. As a positive control, human catestatin (CHGA[352–372]) completely abrogated nicotine's effect (Figure 4b, left). By contrast, synthetic CHGB peptides had little or no effect on catecholamine

release when stimulated by membrane depolarization (Figure 4b, middle), suggesting an element of nicotinic pathway specificity for the secretory effect.

Potency and efficacy of CHGB peptide CHGB[60–67] (KFEVRLLR) to inhibit nicotinic cholinergic-stimulated catecholamine secretion, as well as its cationic signal transduction in chromaffin cells

The inhibitory effect of CHGB[60–67] on nicotinic cholinergic secretion was dose-dependent in PC12 cells. The potency (IC[50]) was 4 μM for CHGB[60–67], versus 0.45 μM for catestatin, while the efficacy (maximal effect, at 10 μM peptide) was ~49% inhibiton for CHGB[60–67] versus ~100% for catestatin (Figure 4b, right). Nicotine stimulated uptake of $^{45}Ca^{2+}$, an effect strongly (~82%) inhibited by catestatin, and moderately (~22%) inhibited by CHGB[60–67] (p<0.0001, Figure 4c). The inhibitory peptide sequence, CHGB[60–67] ($K_{60}FEVRLLR_{67}$), was 100% (i.e., perfectly) conserved across human (P05060), rat (O35314), and mouse (P16014) CHGB protein sequences (UniProt identifiers <http://www.uniprot.org>). This oligopeptide region is located within an amphiphilic domain (similar to the CHGA fragment catestatin) ([33]), and more specifically within an amphiphilic helical (or coiled-coil) patch, as previously described for both CHGA and CHGB ([34]).

Endoproteolytic cleavage of CHGB in the region of the active secretory peptide

We analyzed plasmin-liberated human CHGB peptides by LC-MS/MS, to position the cleavage sites for this chromaffin cell endoproteolytic system. In the region of the active peptide (Table 1A), extensive cleavage was noted, primarily at monobasic sites (i.e., R or K), though also at dibasic site $R_{46}K_{47}$. As a control to explore endoprotease cleavage targets elsewhere in CHGB, we also evaluated a region ($CHGB_{565-596}$) containing three dibasic sites – $K_{566}R_{567}$, $K_{578}R_{579}$, and $R_{595}K_{596}K_{597}$ – that bound two putative peptides for liberation ($CHGB_{568-577}$ and $CHGB_{580-594}$); each of these three dibasic sites was utilized by plasmin, and the expected peptides were formed (Table 1B).

DISCUSSION

Overview

The chromogranin/secretogranin acidic proteins are mainly located within neuroendocrine secretory vesicles such as chromaffin granules and large dense-core vesicles (LDCVs) of monoaminergic neurons ([1,2]). In these organelles, chromogranins constitute the main protein component of the intravesicular matrix. An important property of chromogranins is their ability to bind solutes, thereby allowing LDCVs to accumulate large amounts of catecholamines while maintaining their osmotic stability([35,36]), an effect essential for the maintenance of neurosecretory activity. Several functions have been proposed for chromogranin B (CHGB), including granule biogenesis and sorting ([7,10]), Ca^{2+} sequestration and release ([37]), and a source of bioactive peptides ([38,39]). Alterations in CHGB expression accompany several human diseases of disordered neurotransmitter storage or release, such as hypertension ([18,19,40]), schizophrenia ([41,42]), and Alzheimer disease ([43]). While previous studies of CHGB abundance suggested alterations in storage granule abundance, quantitative studies of physiological processes underpinning

catecholamine synthesis, uptake, storage, and secretagogue-triggered release have been lacking.

CHGB under- and over-expression in catecholaminergic cells, as well as *in vivo*

In PC12 cells, si-RNA silencing successfully diminished CHGB protein expression, with consequent reduction of chromaffin granule abundance, uptake of exogenous catecholamines, and secretagogue-stimulated catecholamine release (Figure 1e). Conversely, expression viral transduction successfully increased CHGB expression, with an increase in chromaffin granule abundance, but only minor changes in cellular ability to uptake catecholamines or respond to secretory stimulation (Figure 3d). Thus, the range of CHGB concentrations between physiological and zero have profound consequences for catecholamine metabolism, while elevation of CHGB beyond the physiological range does influence granule morphogenesis, but seems to have fewer physiological effects, suggesting a sufficient or saturating CHGB concentration under basal circumstances.

Both we (Figure 1b) and Diaz-Vera et al [22] found changes in expression of other chromaffin cell mRNAs during diminution of *CHGB* expression, especially over-expression of *Chga* mRNA. We speculate that such an increase may have dampened the already impressive consequences of CHGB depletion (Figure 1e). Diaz-Vera et al [22] noted diminished adrenal medullary storage of epinephrine and norepinephrine, consistent with our finding of decreased catecholamine uptake capacity (Figure 1e).

In vivo (targeted ablation of the mouse *CHGB* locus), we found similar changes in granule morphology (Figure 2a), with apparently unregulated catecholamine release (Figure 2b), which may underlie the substantially elevated BP observed in the *CHGB*(−/−) mouse [18]. Of note, we previously observed similar catecholamine release and BP effects in the *Chga* knockout mouse [28].

Using an expressed frog CHGA (fCHGA) cDNA and a non-chromaffin cell line (COS-7), Montero-Hadjadje, et al demonstrated that CHGA has the intrinsic capacity to induce formation of mobile secretory granules and to promote the sorting and release of peptide hormones [44]. Our finding of a role for CHGB on the biogenesis of dense core granules (in chromaffin and PC12 cells) indicate that these two homologous proteins exert similar functions.

CHGB peptide regions on catecholamine release

The CHGA peptide catestatin (human CHGA[352–372]) inhibits the physiological (nicotinic cholinergic) pathway of catecholamine release in chromaffin cells [28,29] and polymorphisms in the human catestatin region are associated with risk of hypertension [45]. Here we observed a similar (though less potent) inhibitory effect on nicotinic stimulated secretion for CHGB and its proteolytic fragments (Figure 4a). We then synthesized several peptides that potentially mimic the effects of catestatin, and found that such peptides can inhibit nicotinic cholinergic-stimulated catecholamine release (Figure 4b left) and cationic signal transduction (Figure 4c) in chromaffin cells, albeit at lower potency and efficacy than catestatin. The complete lack of effect of CHGB synthetic peptides on catecholamine

secretion triggered by membrane depolarization (Figure 4b center) reinforces the specificity of such peptides for the nicotinic cholinergic pathway.

The active human CHGB region is completely conserved across mammalian species (human, rat, mouse), and the target region is extensively cleaved by the chromaffin cell plasmin endoproteolytic system (Table 1A), though we have not yet positioned the precise boundaries of the active peptide as formed *in vivo*; as a control, the same system exerts the expected cleavage pattern on multiple dibasic sites in the human CHGB substrate (Table 1B). A more extensive synthetic peptide scan across the entire CHGB protein (or its highly conserved regions) could better establish the active region(s) of the protein.

Conclusions and perspectives

Within chromaffin cells, CHGB participates in assembly of catecholamine secretory vesicles (dense-core granules), and governs the secretory capacity of these granules under the nicotinic stimulation. After proteolytic cleavage and release into the extracellular space, CHGB (and particularly its peptide hCHGB[60–67]) seems to exert a negative feedback effect to inhibit the physiological secretory response to acetylcholine. The autocrine effects of released/processed CHGB on secretion (Figure 5) would be most likely to occur on chromaffin cells, whose chromaffin granules (or LDV [large dense core vesicles]) typically contain both chromogranins and catecholamines, though even sympathetic nerve termini which contain substantial numbers of SDVs (small dense core vesicles, without chromogranins) also harbor some chromogranin-bearing LDVs ([46]).

Derangements of CHGB expression may thus lead to impaired catecholamine storage, with consequently elevated constitutive catecholamine release, eventuating in systemic hypertension. Our data provide direct bi-directional evidence implicating CHGB in vesicular storage of catecholamines, and also novel evidence implicating released CHGB in control of exocytosis. Thus CHGB emerges as a multi-functional protein/peptide, with both intra-cellular and extracellular activities (Figure 5), whose novel properties may contribute to a spectrum of catecholaminergic disease states.

Supplementary Material

Refer to Web version on PubMed Central for supplementary material.

Acknowledgments

Glossary of abbreviations

BP	Blood pressure
CHGA	Chromogranin A
CHGB	Chromogranin B (human: CHGB; rodent: CHGB)
cPPT	central polypurine tract

|	
DBP	Diastolic blood pressure
HBSS	Hank's Balanced Salt Solution
hCHGB	Human CHGB
HR	Heart rate
hPGK	Human phosphoglycerate kinase
HPLC-ECD	high performance liquid chromatography coupled to an electrochemical detection
IPTG	Isopropylβ-D-1-thiogalactopyranoside
KO	Knock-out
LC-MS/MS	C-18 reverse-phase Liquid Chromatography, followed by tandem Mass Spectroscopy
LDCV	large dense-core vesicle
LTR	Long terminal repeat
M.O.I.	Multiplicity of infection
PCR	Polymerase chain reaction
PC12	Rat pheochromocytoma cell line
QTL	Quantitative Trait Locus
siRNA	Small interfering RNA
SBP	Systolic blood pressure
T2A	2A peptide, self-cleavage
TEM	Transmission electron microscopy
UTR	Untranslated region
VSV	Vesicular stomatitis virus
WPRE	Woodchuck hepatitis virus Posttranscriptional Regulatory Element

REFERENCES

1. Huttner WB, Gerdes HH, Rosa P. The granin (chromogranin/secretogranin) family. Trends Biochem Sci. 1991; 16:27–30. [PubMed: 2053134]

2. Taupenot L, Harper KL, O'Connor DT. The chromogranin-secretogranin family. N Engl J Med. 2003; 348:1134–1149. [PubMed: 12646671]

3. Rosa P, Hille A, Lee RW, Zanini A, De Camilli P, Huttner WB. Secretogranins I and II: two tyrosine-sulfated secretory proteins common to a variety of cells secreting peptides by the regulated pathway. J Cell Biol. 1985; 101:1999–2011. [PubMed: 4055903]

4. Falkensammer G, Fischer-Colbrie R, Winkler H. Biogenesis of chromaffin granules: incorporation of sulfate into chromogranin B and into a proteoglycan. J Neurochem. 1985; 45:1475–1480. [PubMed: 4045458]

5. O'Connor DT, Frigon RP, Sokoloff RL. Human chromogranin A. Purification and characterization from catecholamine storage vesicles of human pheochromocytoma. Hypertension. 1984; 6:2–12. [PubMed: 6693145]

6. Schober M, Fischer-Colbrie R, Schmid KW, Bussolati G, O'Connor DT, Winkler H. Comparison of chromogranins A, B, and secretogranin II in human adrenal medulla and pheochromocytoma. Lab Invest. 1987; 57:385–391. [PubMed: 3669614]

7. Huh YH, Jeon SH, Yoo SH. Chromogranin B-induced secretory granule biogenesis: comparison with the similar role of chromogranin A. J Biol Chem. 2003; 278:40581–40589. [PubMed: 12902350]

8. Gill BM, Barbosa JA, Dinh TQ, Garrod S, O'Connor DT. Chromogranin B: isolation from pheochromocytoma, N-terminal sequence, tissue distribution and secretory vesicle processing. Regul Pept. 1991; 33:223–235. [PubMed: 1882087]

9. Karlsson E, Stridsberg M, Sandler S. Chromogranin-B regulation of IAPP and insulin secretion. Regul Pept. 2000; 87:33–39. [PubMed: 10710286]

10. Natori S, Huttner WB. Chromogranin B (secretogranin I) promotes sorting to the regulated secretory pathway of processing intermediates derived from a peptide hormone precursor. Proc Natl Acad Sci U S A. 1996; 93:4431–4436. [PubMed: 8633084]

11. Binder A. A review of the genetics of essential hypertension. Curr Opin Cardiol. 2007; 22:176–184. [PubMed: 17413273]

12. Greenwood TA, Cadman PE, Stridsberg M, et al. Genome-wide linkage analysis of chromogranin B expression in the CEPH pedigrees: implications for exocytotic sympathochromaffin secretion in humans. Physiol Genomics. 2004; 18:119–127. [PubMed: 15138309]

13. Greenwood TA, Rao F, Stridsberg M, et al. Pleiotropic effects of novel trans-acting loci influencing human sympathochromaffin secretion. Physiol Genomics. 2006; 25:470–479. [PubMed: 16554546]

14. O'Connor DT, Takiyyuddin MA, Printz MP, et al. Catecholamine storage vesicle protein expression in genetic hypertension. Blood Press. 1999; 8:285–295. [PubMed: 10803489]

15. Schober M, Howe PR, Sperk G, Fischer-Colbrie R, Winkler H. An increased pool of secretory hormones and peptides in adrenal medulla of stroke-prone spontaneously hypertensive rats. Hypertension. 1989; 13:469–474. [PubMed: 2566578]

16. Takiyyuddin MA, De Nicola L, Gabbai FB, et al. Catecholamine secretory vesicles. Augmented chromogranins and amines in secondary hypertension. Hypertension. 1993; 21:674–679. [PubMed: 8491501]

17. Lillie EO, O'Connor DT. Early phenotypic changes in hypertension: a role for the autonomic nervous system and heredity. Hypertension. 2006; 47:331–333. [PubMed: 16446388]

18. Zhang K, Rao F, Rana BK, et al. Autonomic function in hypertension: Role of genetic variation at the catecholamine storage vesicle protein chromogranin B (CHGB). Circ Cardiovasc Genet. 2009; 2:46–56. [PubMed: 20011129]

19. Zhang K, Rao F, Wang L, et al. Common functional genetic variants in catecholamine storage vesicle protein promoter motifs interact to trigger systemic hypertension. J Am Coll Cardiol. 2010; 55:1463–1475. [PubMed: 20359597]

20. Biswas N, Vaingankar SM, Mahata M, et al. Proteolytic cleavage of human chromogranin a containing naturally occurring catestatin variants: differential processing at catestatin region by plasmin. Endocrinology. 2008; 149:749–757. [PubMed: 17991725]

21. Courel M, Rodemer C, Nguyen ST, et al. Secretory granule biogenesis in sympathoadrenal cells: identification of a granulogenic determinant in the secretory prohormone chromogranin A. J Biol Chem. 2006; 281:38038–38051. [PubMed: 17032650]

22. Diaz-Vera J, Morales YG, Hernandez-Fernaud JR, et al. Chromogranin B gene ablation reduces the catecholamine cargo and decelerates exocytosis in chromaffin secretory vesicles. J Neurosci. 2010; 30:950–957. [PubMed: 20089903]

23. Tiscornia G, Singer O, Verma IM. Production and purification of lentiviral vectors. Nat Protoc. 2006; 1:241–245. [PubMed: 17406239]

24. Taylor CV, Taupenot L, Mahata SK, et al. Formation of the catecholamine release-inhibitory peptide catestatin from chromogranin A. Determination of proteolytic cleavage sites in hormone storage granules. J Biol Chem. 2000; 275:22905–22915. [PubMed: 10781584]

25. Jiang Q, Taupenot L, Mahata SK, et al. Proteolytic cleavage of chromogranin A (CgA) by plasmin. Selective liberation of a specific bioactive CgA fragment that regulates catecholamine release. J Biol Chem. 2001; 276:25022–25029. [PubMed: 11342539]

26. Parmer RJ, Mahata M, Gong Y, et al. Processing of chromogranin A by plasmin provides a novel mechanism for regulating catecholamine secretion. J Clin Invest. 2000; 106:907–915. [PubMed: 11018079]

27. Conlon JM, Hamberger B, Grimelius L. Isolation of peptides arising from the specific posttranslational processing of chromogranin A and chromogranin B from human pheochromocytoma tissue. Peptides. 1992; 13:639–644. [PubMed: 1437706]

28. Mahapatra NR, O'Connor DT, Vaingankar SM, et al. Hypertension from targeted ablation of chromogranin A can be rescued by the human ortholog. J Clin Invest. 2005; 115:1942–1952. [PubMed: 16007257]

29. Mahata SK, Mahata M, Parmer RJ, O'Connor DT. Desensitization of catecholamine release. The novel catecholamine release-inhibitory peptide catestatin (chromogranin a344–364) acts at the receptor to prevent nicotinic cholinergic tolerance. J Biol Chem. 1999; 274:2920–2928. [PubMed: 9915830]

30. Wegrzyn JL, Bark SJ, Funkelstein L, et al. Proteomics of dense core secretory vesicles reveal distinct protein categories for secretion of neuroeffectors for cell-cell communication. J Proteome Res. 2010; 9:5002–5024. [PubMed: 20695487]

31. Gupta N, Bark SJ, Lu WD, et al. Mass spectrometry-based neuropeptidomics of secretory vesicles from human adrenal medullary pheochromocytoma reveals novel peptide products of prohormone processing. J Proteome Res. 2010; 9:5065–5075. [PubMed: 20704348]

32. Hook V, Bark S, Gupta N, et al. Neuropeptidomic components generated by proteomic functions in secretory vesicles for cell-cell communication. AAPS J. 2010; 12:635–645. [PubMed: 20734175]

33. Kennedy BP, Mahata SK, O'Connor DT, Ziegler MG. Mechanism of cardiovascular actions of the chromogranin A fragment catestatin in vivo. Peptides. 1998; 19:1241–1248. [PubMed: 9786174]

34. Mosley CA, Taupenot L, Biswas N, et al. Biogenesis of the secretory granule: chromogranin A coiled-coil structure results in unusual physical properties and suggests a mechanism for granule core condensation. Biochemistry. 2007; 46:10999–11012. [PubMed: 17718510]

35. Videen JS, Mezger MS, Chang YM, O'Connor DT. Calcium and catecholamine interactions with adrenal chromogranins. Comparison of driving forces in binding and aggregation. J Biol Chem. 1992; 267:3066–3073. [PubMed: 1737762]

36. Helle KB, Reed RK, Pihl KE, Serck-Hanssen G. Osmotic properties of the chromogranins and relation to osmotic pressure in catecholamine storage granules. Acta Physiol Scand. 1985; 123:21–33. [PubMed: 3969832]

37. Yoo SH, Jeon CJ. Inositol 1,4,5-trisphosphate receptor/Ca2+ channel modulatory role of chromogranin A. a Ca2+ storage protein of secretory granules. J Biol Chem. 2000; 275:15067–15073. [PubMed: 10748130]

38. Strub JM, Garcia-Sablone P, Lonning K, et al. Processing of chromogranin B in bovine adrenal medulla. Identification of secretolytin, the endogenous C-terminal fragment of residues 614–626 with antibacterial activity. Eur J Biochem. 1995; 229:356–368. [PubMed: 7744058]

39. Winkler H, Laslop A, Leitner B, Weiss C. The secretory cocktail of adrenergic large dense-core vesicles: the functional role of the chromogranins. Adv Pharmacol. 1998; 42:257–259. [PubMed: 9327893]

40. Zhang K, Chen Y, Wen G, et al. Catecholamine storage vesicles: role of core protein genetic polymorphisms in hypertension. Curr Hypertens Rep. 2011; 13:36–45. [PubMed: 21104344]

41. Landen M, Grenfeldt B, Davidsson P, et al. Reduction of chromogranin A and B but not C in the cerebrospinal fluid in subjects with schizophrenia. Eur Neuropsychopharmacol. 1999; 9:311–315. [PubMed: 10422891]

42. Marksteiner J, Lechner T, Kaufmann WA, et al. Distribution of chromogranin B-like immunoreactivity in the human hippocampus and its changes in Alzheimer's disease. Acta Neuropathol (Berl). 2000; 100:205–212. [PubMed: 10963369]

43. Marksteiner J, Kaufmann WA, Gurka P, Humpel C. Synaptic proteins in Alzheimer's disease. J Mol Neurosci. 2002; 18:53–63. [PubMed: 11931350]

44. Montero-Hadjadje M, Elias S, Chevalier L, et al. Chromogranin A promotes peptide hormone sorting to mobile granules in constitutively and regulated secreting cells: role of conserved N- and C-terminal peptides. J Biol Chem. 2009; 284:12420–12431. [PubMed: 19179339]

45. Rao F, Wen G, Gayen JR, et al. Catecholamine release-inhibitory peptide catestatin (chromogranin A(352–372)): naturally occurring amino acid variant Gly364Ser causes profound changes in human autonomic activity and alters risk for hypertension. Circulation. 2007; 115:2271–2281. [PubMed: 17438154]

46. O'Connor DT, Klein RL, Thureson-Klein AK, Barbosa JA. Chromogranin A: localization and stoichiometry in large dense core catecholamine storage vesicles from sympathetic nerve. Brain Res. 1991; 567:188–196. [PubMed: 1817725]

Effective silencing of Chgb expression by siRNA in chromaffin cells: Decline in Chgb protein

Chgb immunoblot

Quantification by scan
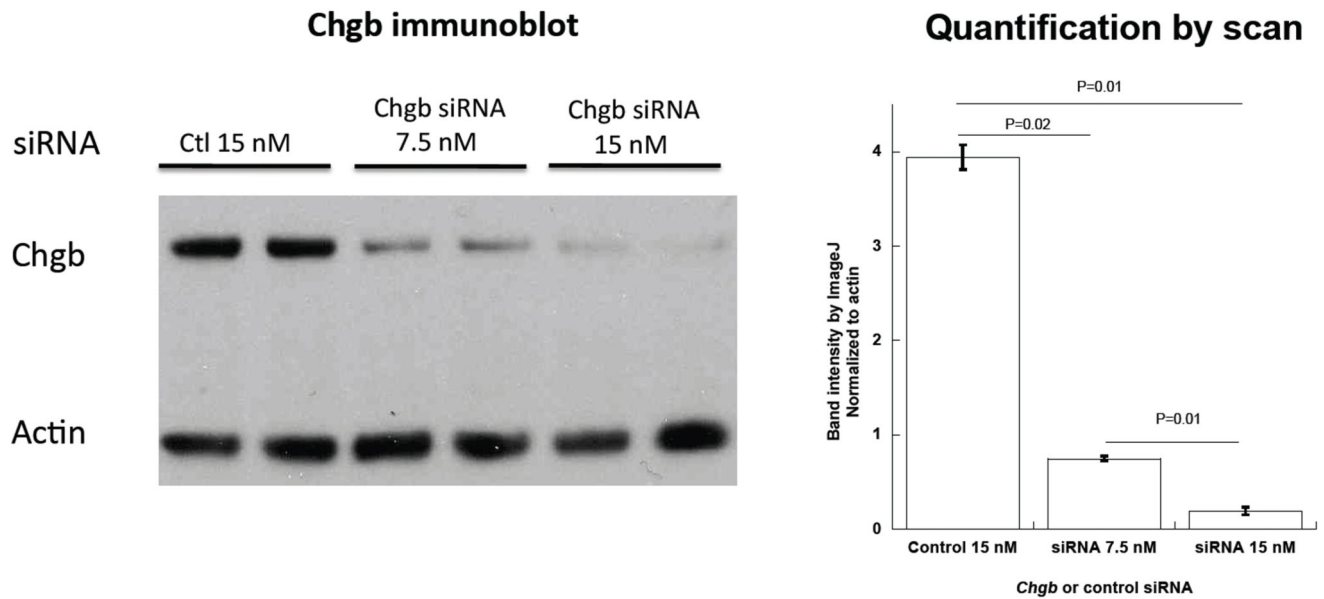
siRNA: siGENOME SMARTpool (Dharmacon)
Transfection: Transfectin (Bio-Rad).
Cells: PC12.
Protein extracted 96 hours after transfection.
Image intensity determination: ImageJ

a

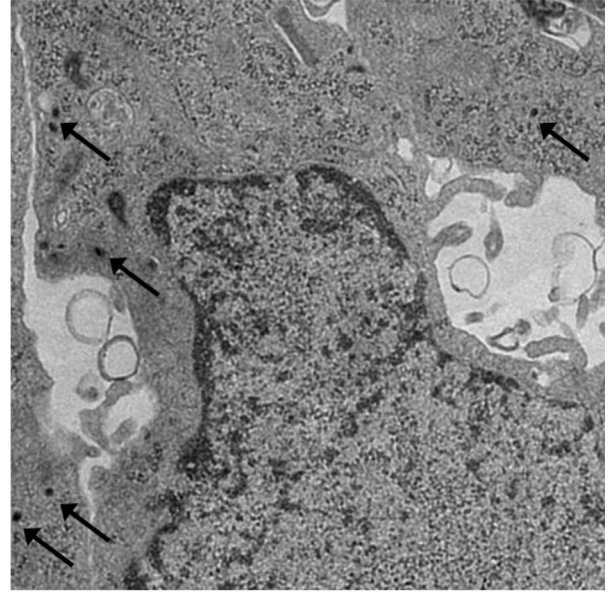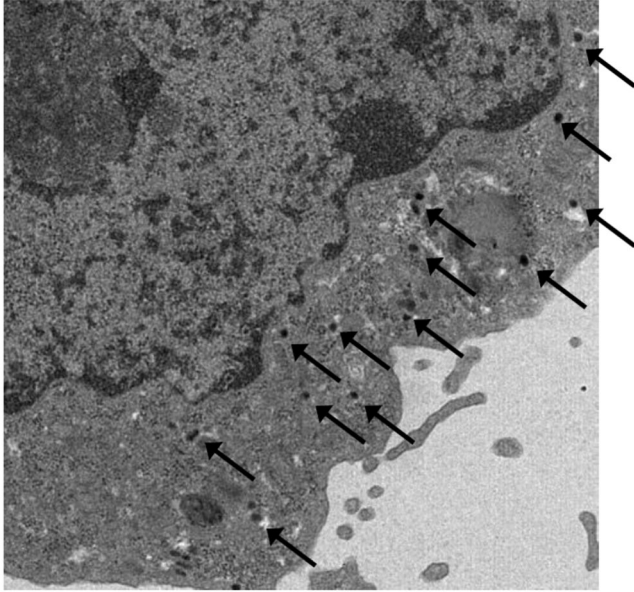**Expression of catecholamine storage and synthesis genes in chromaffin cells with *Chgb* knockdown by siRNA**
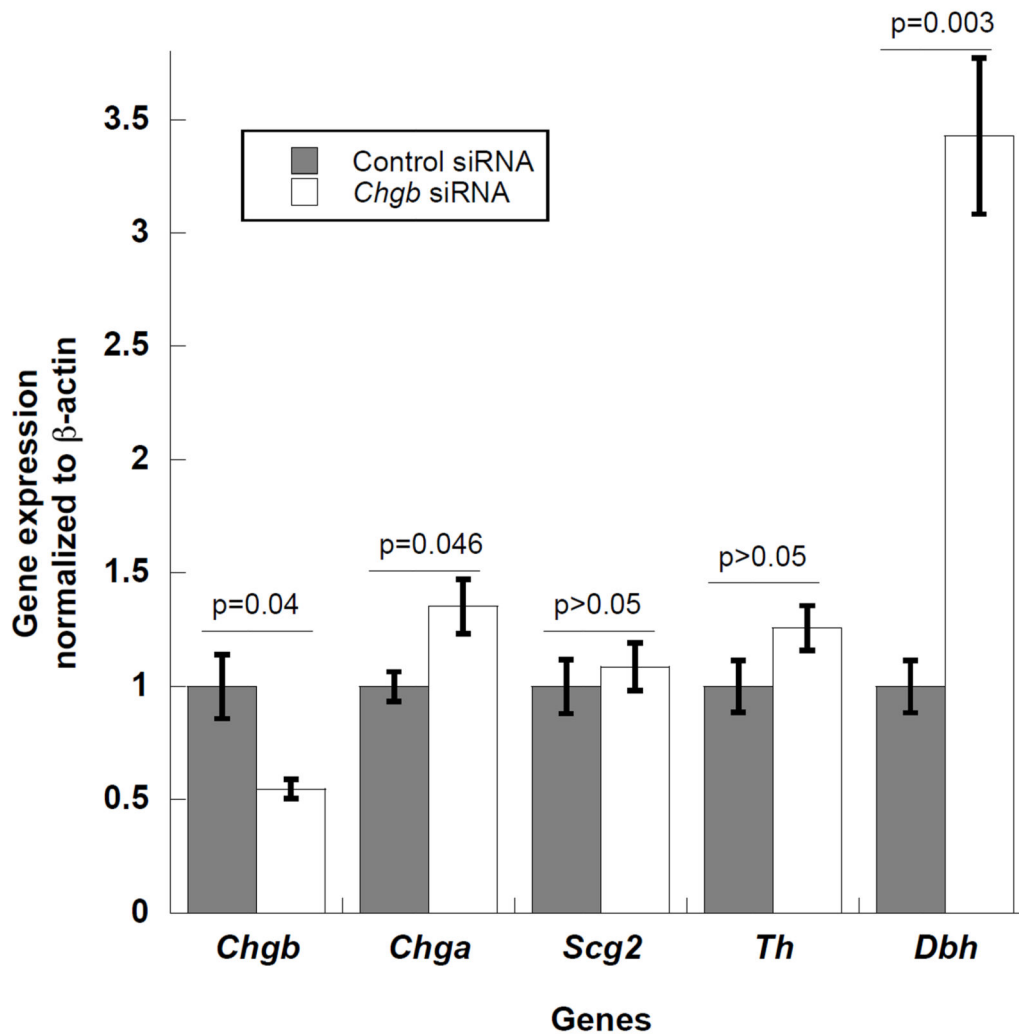
b

Chgb siRNA silencing in rat chromaffin (PC12) cells: Transmission EM
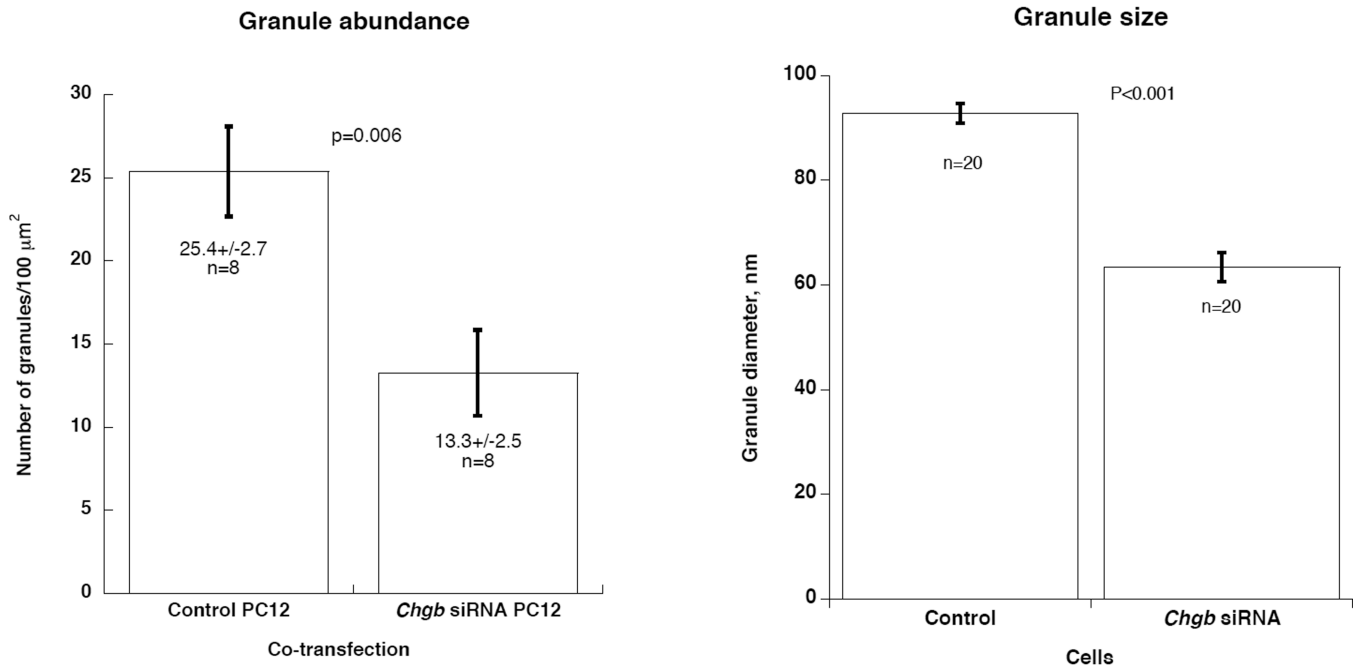
Mock

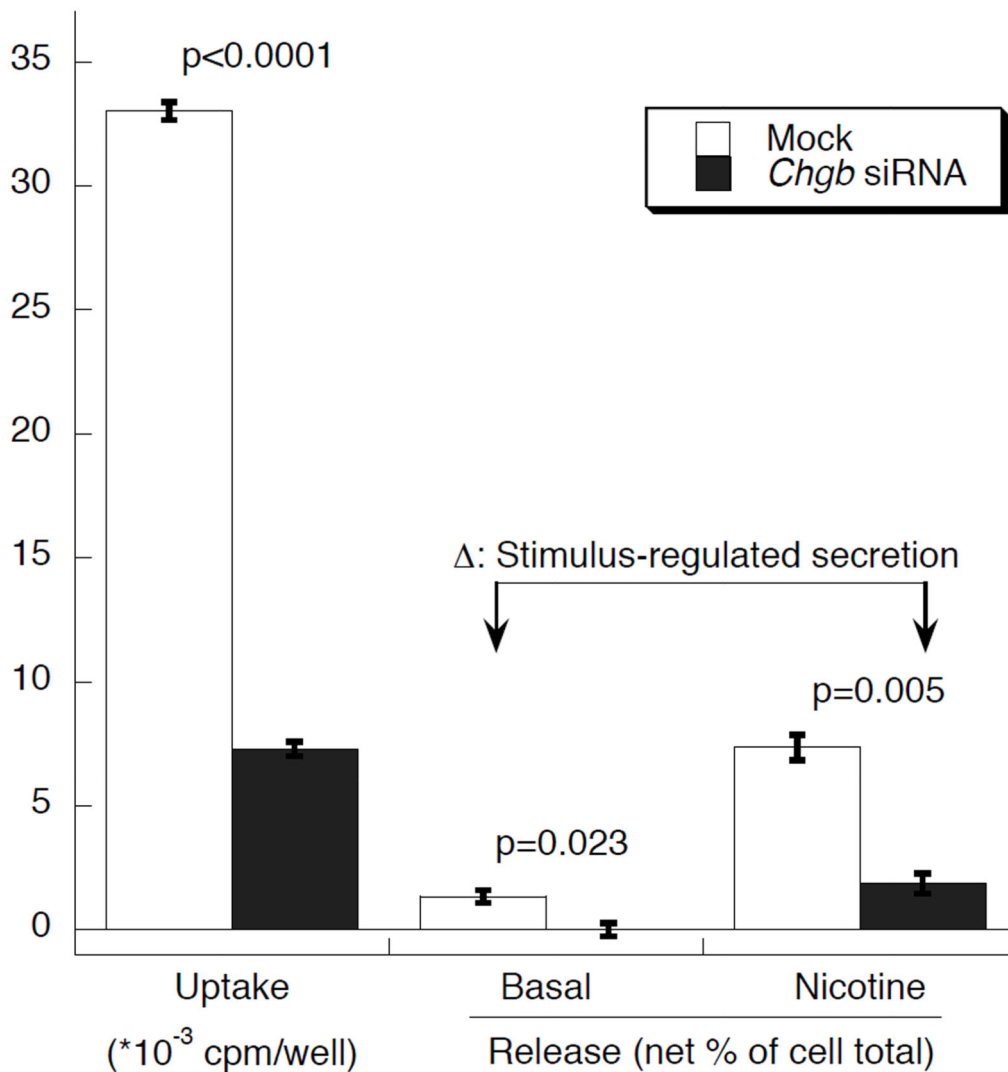**Chgb siRNA**

Bar: 2 μm

↖ : Dense core secretory granules

C

Dense-core chromaffin granules: Abundance quantification and size determination

Granule abundance

Granule size

d

Chgb silencing in chromaffin cells by siRNA:
## Effects on [³H]-L-norepinephrine uptake and release

Figure 1. Under-expression of *CHGB* by siRNA in chromaffin cells
1a. Left: Immunoblot of CHGB protein in siRNA-transfected PC12 cells. The rat *CHGB* siRNA siGENOME "smart pool" was transfected into PC12 cells and silencing of *CHGB* expression was evaluated by immunoblotting at the target protein level. ~95% knockdown of *CHGB* expression was achieved by 15 nM siRNA**. Right: Quantification of CHGB in the blot.** Band intensity was scanned and scored by ImageJ. **1b. Expression of catecholamine pathway (storage, synthesis) genes in *CHGB* siRNA-silenced PC12 cells.** The rat *CHGB* siRNA siGENOME "smart pool" was transfected at 15 nM into PC12 cells and transcript expression was scored by real-time qPCR, and normalized to the signal for β-actin. Each condition was repeated four times. During knockdown, the *CHGB* transcript was

under-expressed, while *Chga* and *Dbh* were over-expressed, but *Scg2* and *Th* were unchanged. **1c. Visualization of dense-core granules in *CHGB* siRNA-silenced PC12 cells by transmission EM.** PC12 cells were transfected with the rat *CHGB* siRNA siGENOME "smart pool" at 15 nM and visualized by Zeiss EM10B electron microscope. CHGB siRNA-silenced PC12 cells display fewer dense-core granules than control (mock-transfected) cells. Arrowheads: Dense core secretory granules. Bar: 2 μm. **1d. Quantification of dense-core chromaffin granule abundance after *CHGB* silencing by siRNA.** The data come from figure 1C. Left, granule number, n=8 cells were counted for each condition. Right, granule diameter, n=20 granules were measured for each condition. **1e. Effect of *CHGB* silencing on exogenous catecholamine uptake and secretagogue-triggered release.** PC12 cells were labeled with [^{3}H]-L-norepinephrine and treated with nicotine at 60 μM. The supernant and cell lysates were collected to measure radioactivity. The uptake was expressed as counts in cell lysate. The percent (%) secretion was expressed as [amount released/(amount released + amount in cell lysate)] $\times$ 100. Each condition was repeated three times. CHGB-silenced PC12 cells displayed diminished uptake of exogenous catecholamine, as well as reduced release catecholamine when stimulated by nicotine.
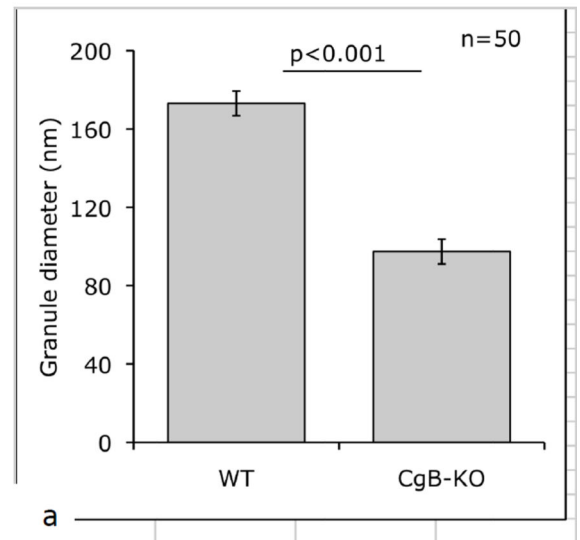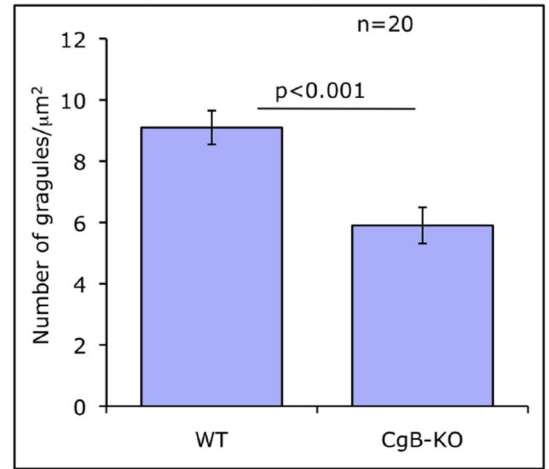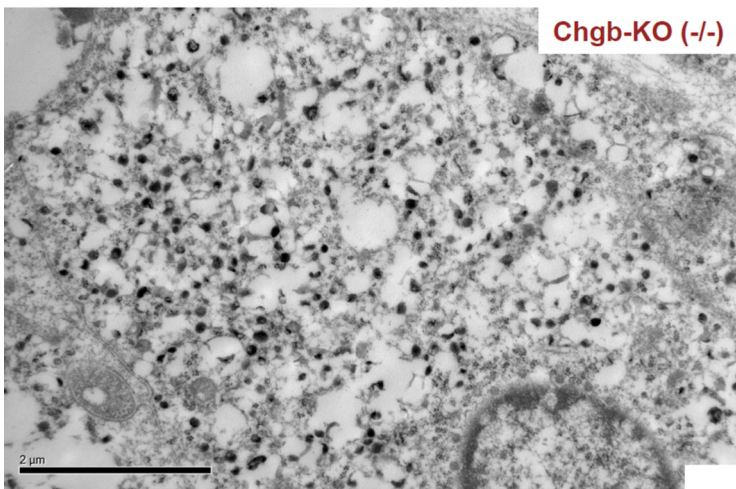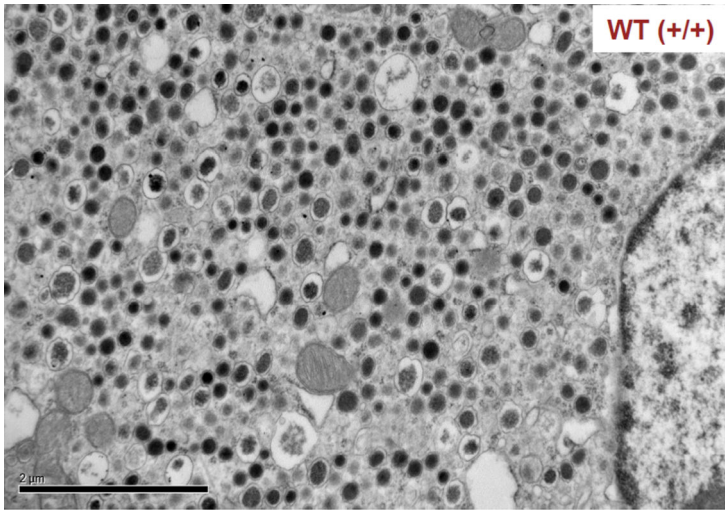
Plasma catecholamines in *Chgb* knockout mice
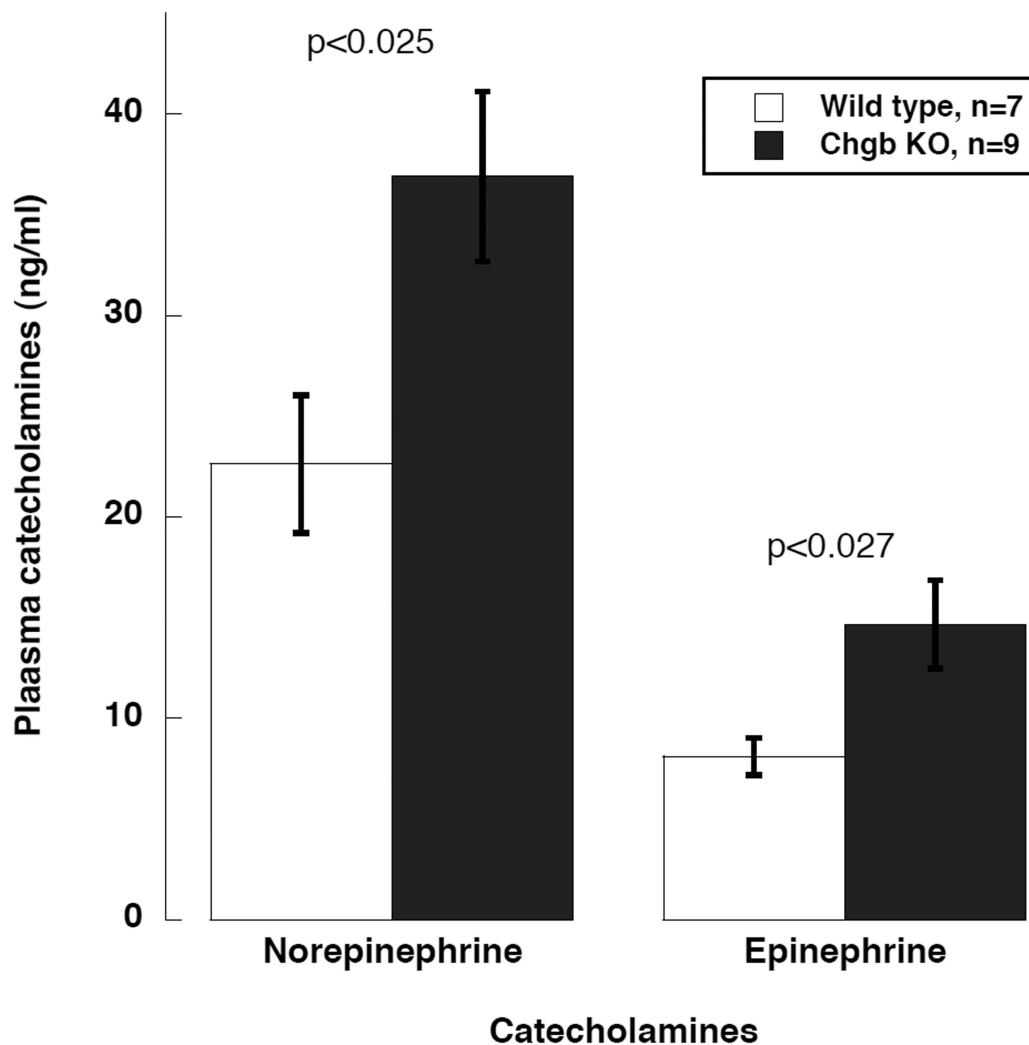
b

Figure 2. Effects of *CHGB* targeted ablation *in vivo*: The *CHGB* ablation (–/–) mouse
2a. Left: Morphology of the adrenal medulla by transmission EM. Visualization of dense-core granules in *CHGB* (+/+; top) versus *CHGB* (–/–; bottom) mice. Bars: 2 μm.
Right: Quantification and diameter determination of dense-core chromaffin granule abundance in *CHGB* (+/+) versus *CHGB* (–/–). Both the number (n=20 cells were counted for each condition) and size of granules (n=20 granules were measured for each condition) declined in *CHGB* (–/–) mice. **2b. Catecholamine secretion during *CHGB* ablation *in vivo*.** Mouse plasma sample were collected and catecholamines were measured by HPLC-ECD system. Both norepinephrine and epinephrine in the circulation increased after *CHGB* ablation. (n=7 for wild type and n=9 for Chgb knockout)

CHGB over-expression in chromaffin cells:
Transduction by human CHGB-expressing lentivirus
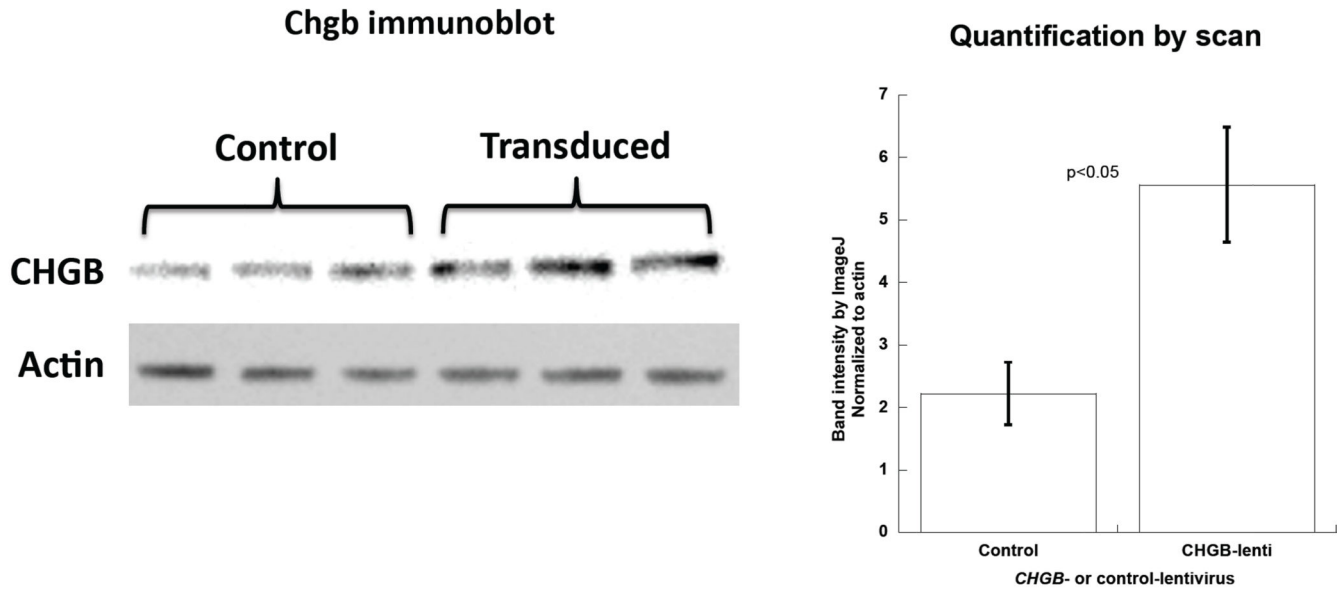
Transduction: Lenti-hPGK-tdTomato-T2A-CHGB
Cells: PC12.
Protein extracted after 96 hours after transduction.

a

Dense-core chromaffin granules in CHGB-lentivirus-transduced chromaffin cells: Transmission EM

Mock

CHGB-expressing lentivirus

—— Bar: 2 μm

↖ : Dense core secretory granules

b

Chromaffin granule abundance during CHGB over-expression
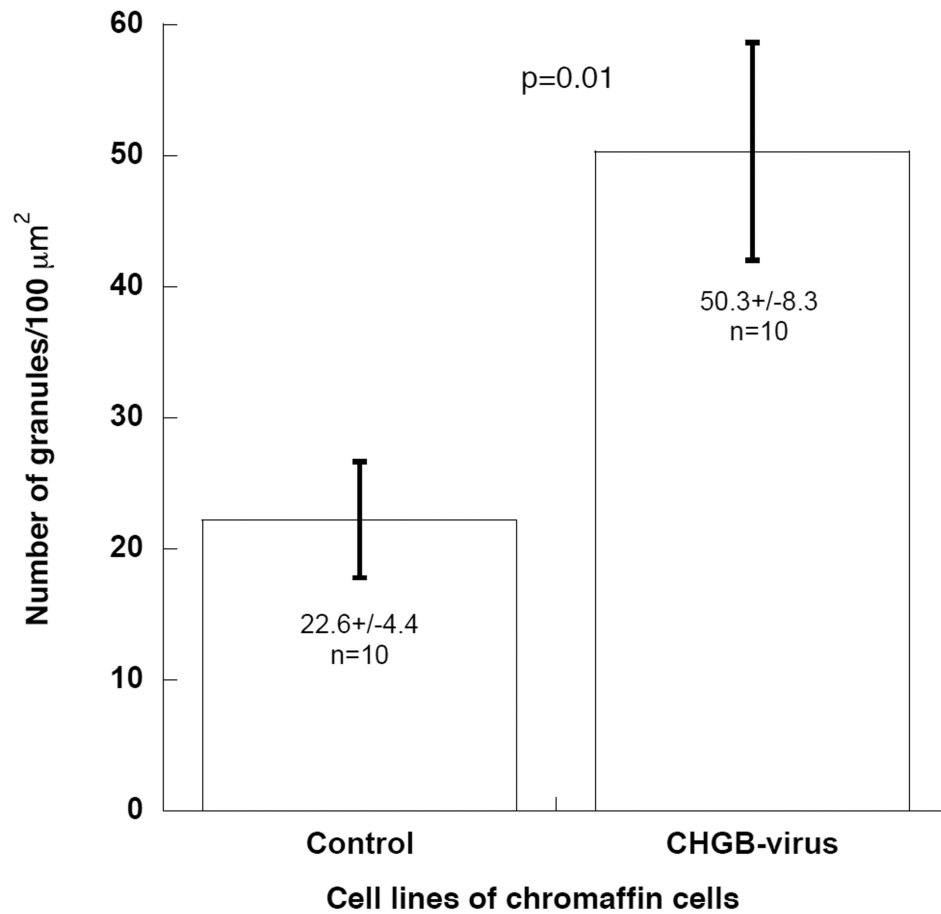
c

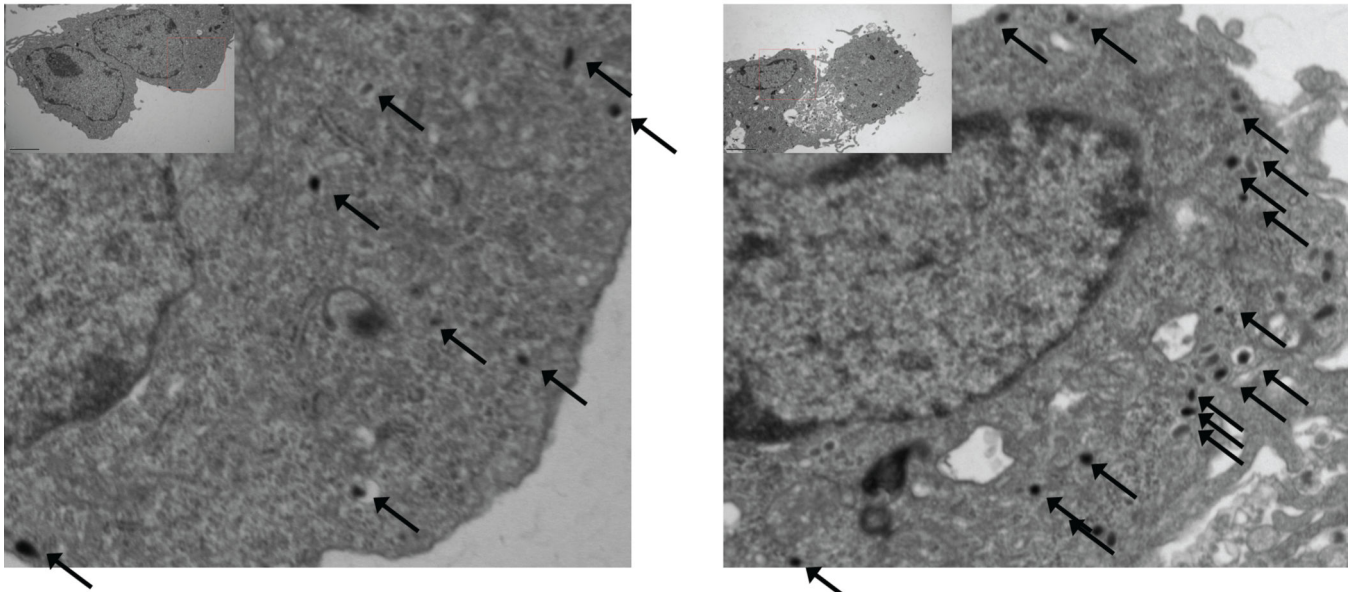## *CHGB* over-expression in chromaffin cells by lentivirus:
Effects on [^{3}H]-L-norepinephrine uptake and release

Mock
CHGB lentivirus

p=0.019

Δ: Stimulus-regulated secretion

p=0.168

p=0.538

Uptake

(*10^{-3} cpm/well)

Basal

Nicotine

Release (net % of cell total)
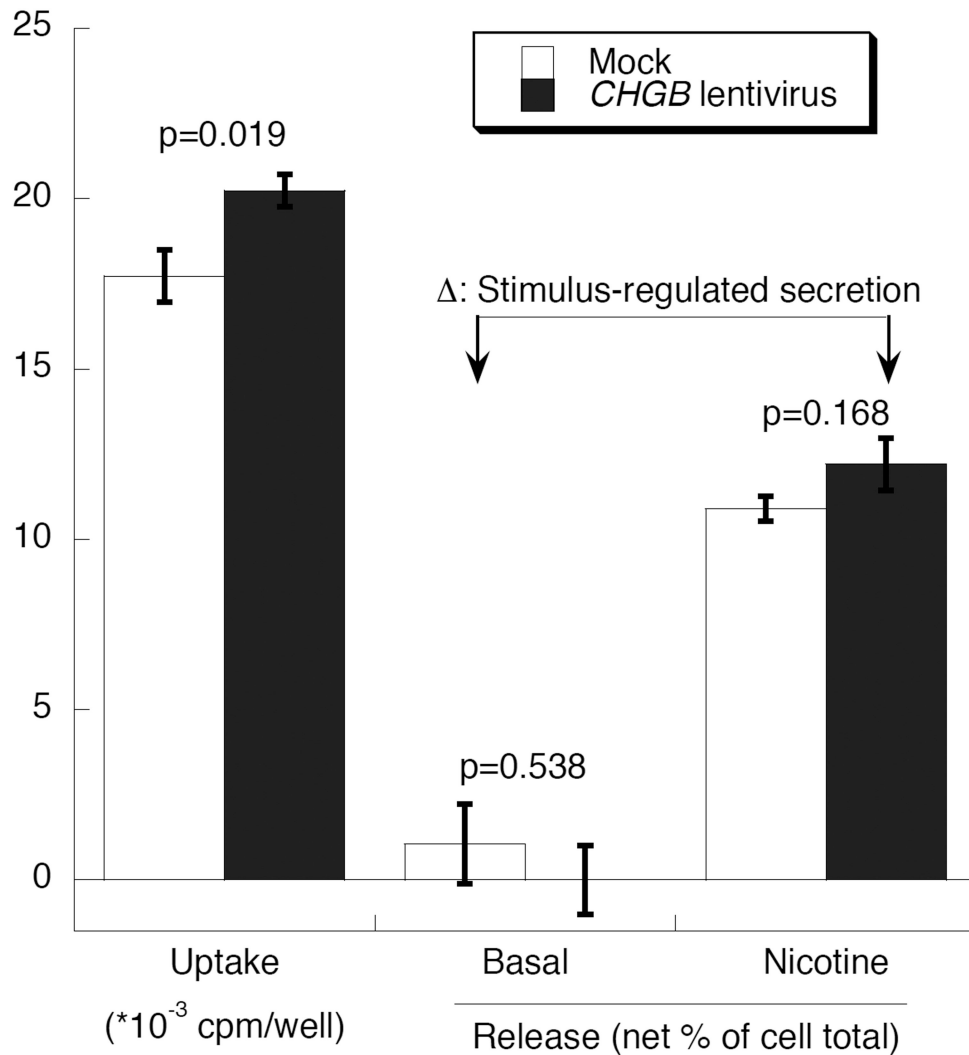
d

Figure 3. Over-expression of *CHGB* by lentiviral transduction in chromaffin cells
3a. Left: Immunoblot of CHGB in human *CHGB*-lentivirus transduced PC12 cells.
Right: Quantification of CHGB by scan. After 48 hours of transduction, CHGB was
quantified by immunoblot with goat polyclonal IgG (sc-1489, Santa Cruz Biotechnology).
Actin was used as a housekeeping probe. A ~150% increase of CHGB protein was achieved
by this transduction. Band intensity was scored by ImageJ. **3b. Visualization of dense-core**
granules in *CHGB*-lentivirus-transduced PC12 cells, by transmission EM. The main/
larger image magnifications are 1/12 of the originals (insets shown in upper left corners).
The magnification of the original image (inset) was 10,000x. The scale bar in the original
(inset) images is 2 μm. Arrowheads: Dense core secretory granules. **3c. Quantification of**
dense-core chromaffin granule abundance in h*CHGB*-lentivirus-transducted PC12
cells. The h*CHGB* transducted PC12 cells display more granules than control PC12 cells

(p=0.01, n=10 cells were counted for each condition). Granule diameter was similar in both cell lines, at 92.8±1.87 nm in control cells and 90.9±2.98 nm in *CHGB* over-expressing cells. **3d. Effect of CHGB over-expression on catecholamine uptake and release in PC12 cells.** Each condition was repeated three times. After the transduction of CHGB-lentivirus, the uptake of exogenous catecholamine increased by ~14%, but nicotine-stimulated secretion did not change.

CHGB: Effect on catecholamine release from chromaffin cells

Nicotinic cholinergic-stimulated release

Overall 1-way ANOVA: F=202, p<0.0001

Bar chart with y-axis "[³H]-L-norepinephrine net secretion, %" (0–25) and x-axis "Condition". Values: Mock ~0; Nicotine 60 µM = 20.06% (p<0.001 vs Mock); Nicotine + CHGB 3 µM = 9.36% (p<0.001); Nicotine + CHGB + Plasmin = 5.57% (p<0.001, p<0.05).

Membrane depolarization-stimulated release

Overall 1-way ANOVA: F=202, p<0.0001

Bar chart with y-axis "[³H]-L-norepinephrine net secretion, %" (0–50) and x-axis "Condition". Values: Mock ~0; KCl 55 mM = 45.1%; KCl +CHGB 3µM = 34.7% (p=0.003); KCl +CHGB +Plasmin = 30.7% (p=0.012).
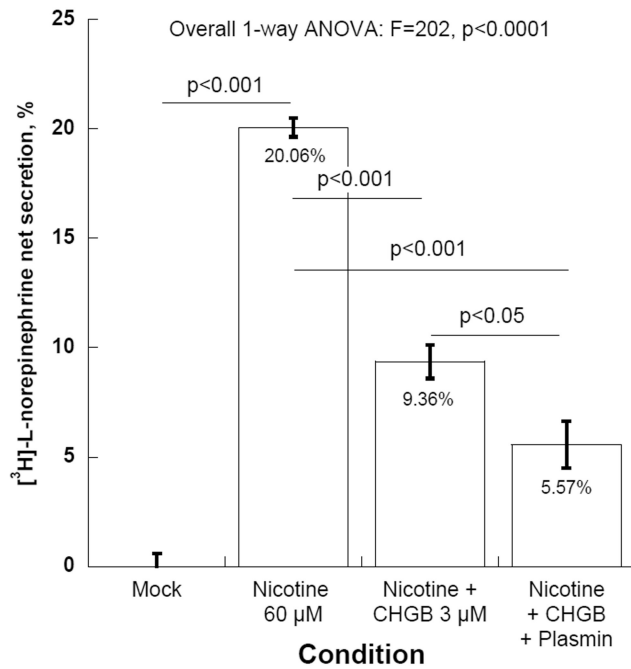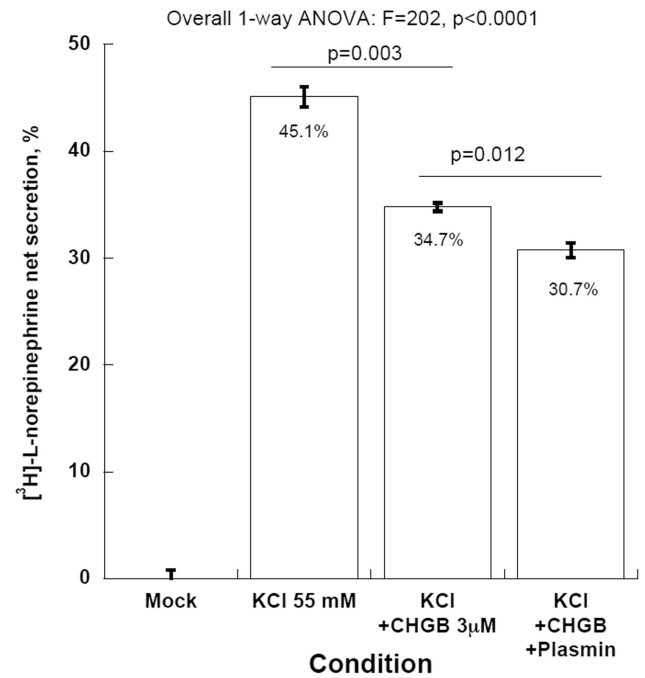
a

CHGB small peptides:
Effect on catecholamine release from chromaffin cells

Nicotinic cholinergic-stimulated release

Net [³H]-norepinephrine secretion stimulated by nicotine (60 µM)

P1: KFEVRLLR
P2: TRPRHHHGRSRPDR
P3: LEWERYRGRGSEEYRAPR
P4: RGLEPGKGRHHRGRGGEPRAYFMSDTREEKR
P5: RFQDKQYSSHHTAEKRKR

p<0.001
p=0.007
p>0.05
p<0.05
p<0.05
p<0.001

Peptides at 10 µM

None, hCHGB[60-67] P1, hCHGB[259-272] P2, hCHGB[337-354] P3, hCHGB[389-419] P4, hCHGB[480-497] P5, hCHGA[352-372] Catestatin

Membrane depolarization-stimulated release

Net [³H]-norepinephrine secretion after membrane depolarization (55 mM KCl)

P1: KFEVRLLR
P2: TRPRHHHGRSRPDR
P3: LEWERYRGRGSEEYRAPR
P4: RGLEPGKGRHHRGRGGEPRAYFMSDTREEKR
P5: RFQDKQYSSHHTAEKRKR

Peptides at 10 µM

None, hCHGB[60-67] P1, hCHGB[259-272] P2, hCHGB[337-354] P3, hCHGB[389-419] P4, hCHGB[480-497] P5, hCHGA[352-372] Catestatin

Potency and efficacy

Net [³H]-norepinephrine secretion stimulated by nicotine (60 µM)

KFEVRLLR (hCHGB[60-67]) P1
Catestatin (hCHGA[352-372])

2-way ANOVA:
Dosage: p<0.001
Peptide: p<0.001
Dosage*peptide: p<0.001

Peptide	Potency (IC[50])	Efficacy (% inhib. @ 10 µM)
hCHGB	4.0 µM	41% inhib.
hCHGA	0.45 µM	100% inhib.

Peptide concentration, µM

b

CHGB peptides and nicotinic cholinergic signal transduction:

Cellular uptake of $^{45}Ca^{2+}$

c
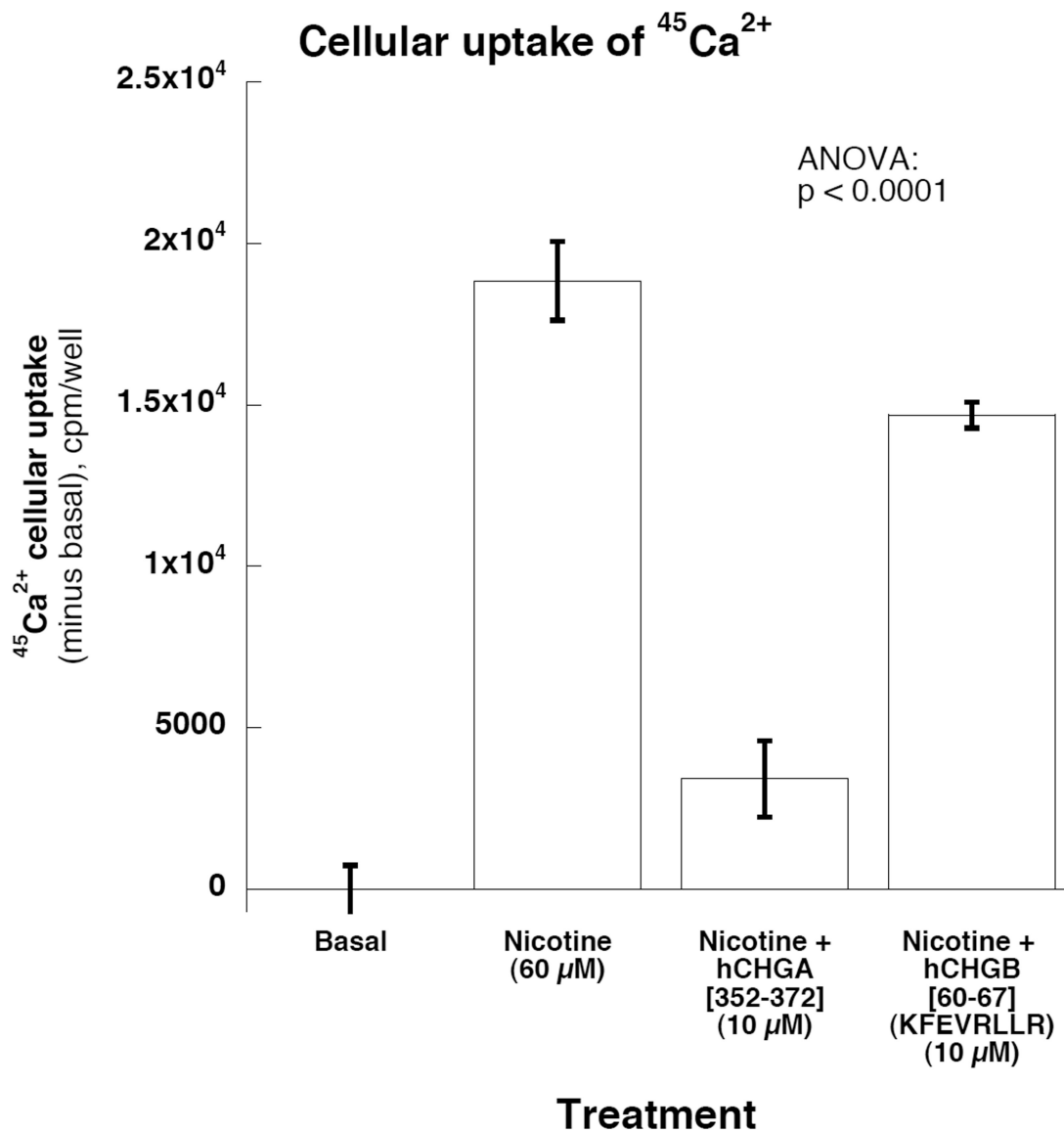
Figure 4. Extracellular CHGB effects on catecholamine release
Each experiment was repeated 3 times.

**4a: Human CHGB protein or its proteolytically-digested fragments on nicotinic cholinergic versus membrane depolarization (KCl) -stimulated catecholamine release.** CHGB protein or its plasmin-digested fragments inhibited predominantly nicotine-stimulated catecholamine release. **4b: Left: Synthetic CHGB peptides on nicotinic cholinergic stimulated catecholamine release.** Catestatin (human CHGA[352–372]) served as a positive inhibitory control. Peptide human CHGB[60–67] displayed the greatest inhibitory effect among these peptides. P value is displayed for each peptide compared with negative control. **Middle: Synthesized Human CHGB peptides on membrane depolarization (KCl)- stimulated catecholamine release.** Catestatin (human CHGA[352–

372]) served as a positive inhibitory control. No inhibitory effect was observed for these peptides (p>0.05 for each peptide).

Right: Potency and efficacy of CHGB[60–67] on nicotinic cholinergic-stimulated catechalmine release. Catestatin (human CHGA[352–372]) served as a positive control. Potency and efficacy of CHGB[60–67] are displayed. **4c: CHGB peptide effect on nicotinic cholinergic cationic (Ca^{2+}) signal transduction in chromaffin cells.** PC12 cells were treated with $^{45}Ca^{2+}$ at 2 μCi/ml and incubated under different conditions including basal, nicotine alone at 60 μM, and nicotine with hCHGA or hCHGB peptides. Catestatin (human CHGA[352–372]) served as a positive control inhibitor. Human CHGB[60–67] moderately (by ~22%) inhibited nicotine-triggered uptake of ^{45}Ca.

Chromogranin B (CHGB): Reciprocal actions on catecholamine storage and release
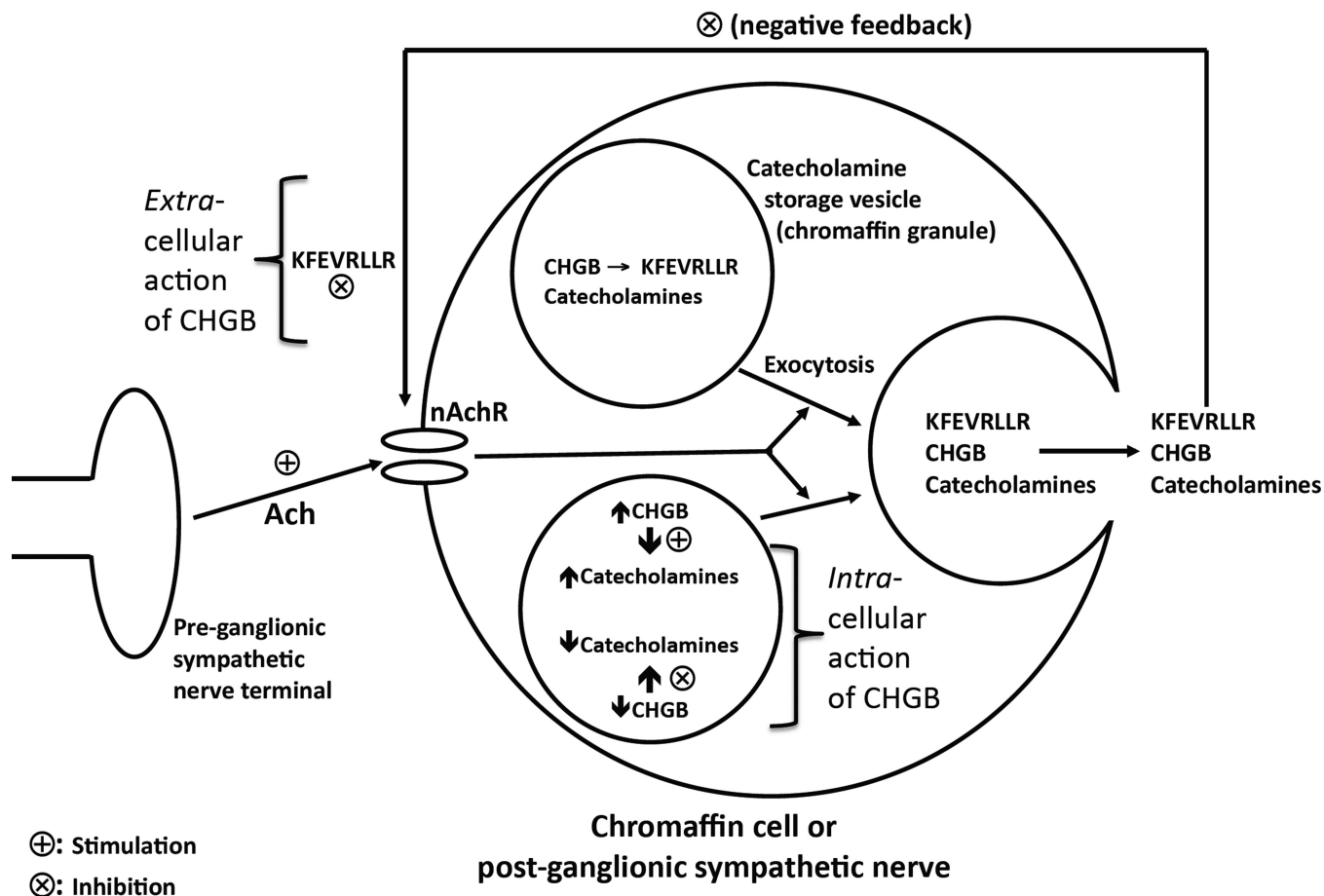
Figure 5. Schema: Reciprocal actions of CHGB on catecholamine storage (stimulation) and release (inhibition)

The figure synthesizes the consequences of our CHGB results for these physiological processes. Within chromaffin cells, CHGB participates in assembly of catecholamine secretory vesicles (dense-core granules), and governs the secretory capacity of these granules under the nicotinic stimulation. After proteolytic cleavage and release into the extracellular space, CHGB (and particularly its peptide hCHGB[60–67]) seems to exert a negative feedback effect to inhibit the secretory response to acetylcholine.

Table 1

Tandem MS on human CHGB after endoproteolytic cleavage by plasmin

Alignments by Clustal Omega (1.2.0).

Legend: *Italics* = paired basic residues; <u>Underlined</u> = Active peptide tested; # Obs = Number of times that peptide was observed in spectra.

```
A. CHGB amino-terminal region harboring the active secretory peptide.

Identified         Sequence                                                              # Obs.
Peptide_1          --VLKTSRKDVKDKETTENENTKFEVR---------------------------------       1
Peptide_2          -----TSRKDVKDKETTENENTKFEVR---------------------------------       19
Peptide_3          -----TSRKDVKDKETTENENTKFEV----------------------------------       6
Peptide_4          -QVLKTSRKDVKDKETTENENTKFEVR---------------------------------       1
Peptide_5          ---------DVKDKETTENENTKFEVR---------------------------------       4
Peptide_6          ------------DKETTENENTKFEV----------------------------------       6
Peptide_7          ------------DKETTENENTKFEVR---------------------------------       3
Peptide_8          ------------DKETTENENTKFEVRL--------------------------------       6
Peptide_9          -----TSRKDVKDKETTENENTKFEVRL--------------------------------       10
Peptide_10         -----TSRKDVKDKETTENENTKFEVRLLRDPADASEAHESSSRGEAGAPGEEDIQGPTK-      2
CHGB_template      CRQVLKTSRKDVKDKETTENENTKFEVRLLRDPADASEAHESSSRGEAGAPGEEDIQGPTKAD    -
                      |         |              |           |            |           |
Residue            40        50             60          70           80           90


B. Small CHGB carboxy-terminal region with three nearby dibasic sites.

Identified      Sequence                           # Obs.
Peptide_1       ---LARVPKLDLKRQYDRVAQLDQLLHY---     3
Peptide_2       ---LARVPKLDLKRQYDR-------------     1
Peptide_3       -RNLARVPKLDLK------------------     3
Peptide_4       --NLARVPKLDL-------------------     6
Peptide_5       --NLARVPKLDLK------------------     13
Peptide_6       --NLARVPKLDLKR-----------------     1
Peptide_7       --NLARVPKLDLKRQYDR-------------     4
Peptide_8       --NLARVPKLDLKRQYDRVAQLDQLLHY---     5
Peptide_9       --NLARVPKLDLKRQYDRVAQLDQLLHYR--     3
Peptide_10      ---LARVPKLDL-------------------     3
Peptide_11      -------------RQYDRVAQLDQLLHY---     7
Peptide_12      -------------QYDRVAQLDQLLHY---      2
Peptide_13      -------------QYDRVAQLDQLLHYR--      5
Peptide_14      -------------RQYDRVAQLDQLLHYR--     8
CHGB_template   KRNLARVPKLDLKRQYDRVAQLDQLLHYRKK    -
                   |         |         |
Residue          570       580       590
```